ACS OMEGA

http://pubs.acs.org/journal/acsodf

Article

Solvation Free Energy for Selection of an Aqueous Two-Phase System: Case in Paeonol Extraction from *Cortex Moutan*

Haiming Huang, Xiaojing Mu,* Jing Deng, Shangyou Xiao, Zhiwei Luo, and Gang Chen

Cite This: *ACS Omega* 2022, 7, 30920−30929

Read Online

ACCESS | Metrics & More | Article Recommendations | Supporting Information

ABSTRACT: Aqueous two-phase system(s) (ATPS) has/have been widely employed in the extraction and separation of bioactive molecules from herbs due to its various advantages such as high efficiency and good selectivity. For selecting the type and amount of organics and salts in ATPS, onerous experimental trials are required to ensure the reliability. We intended to develop a theoretical method to select ATPS in the case of paeonol extraction from *cortex moutan*. The solvation free energies (E_{solv}) of paeonol in the top phase of 54 ATPS (ATPS-acetone, ATPS-acetone-EA, ATPS-THF, ATPS-THF-EA, ATPS-EtOH, and ATPS-EtOH-EA) were calculated with Gaussian 09, and the extraction yields with 54 ATPS were determined. By comparison of E_{solv} and yield, the E_{solv} rank was effective to select the optimal organic type and organic solvent fraction and aqueous salt concentration. With each series of 18 ATPS (ATPS-acetone plus ATPS-acetone-EA; ATPS-THF plus ATPS-THF-EA; or ATPS-EtOH plus ATPS-EtOH-EA), the paeonol yield was correlated with E_{solv}, suggesting that the optimal organic type and fraction and the aqueous NaH_2PO_4 concentration could be selected by using theoretical E_{solv}, or at least, the theoretical E_{solv} rank could offer effective guidance for experimental design, and thus, tedious and onerous experimental work for optimization in ATPS extraction can be significantly reduced.

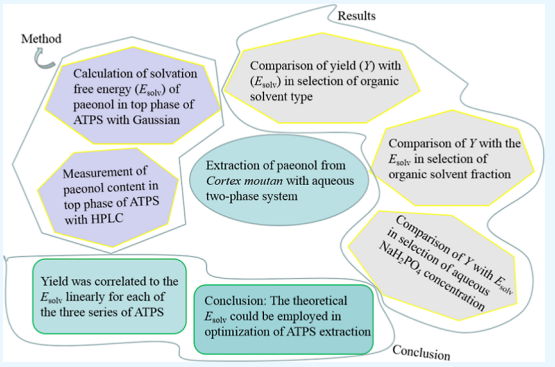

INTRODUCTION

Aqueous two-phase system(s) (ATPS) is/are generally formed by the addition of two (or more) incompatible water-soluble components (*e.g.*, polymers, ionic liquids, water-miscible organics, and salts, among others) into water with concentrations exceeding the critical points.[1−4] Additionally, the rising three-liquid-phase system (TLPS) for extraction and purification was usually formed by adding a hydrophobic phase to ATPS. ATPS and its derivative TLPS attracted tremendous interest to researchers for extraction, separation, purification, and enrichment of proteins[5,6] and active components from herbs[7−10] in various scientific fields such as the food industry, biomedical engineering, pharmaceutical engineering, wet metallurgy, and so on. For example, ATPS were employed for fractionation of micro-algal biomolecules[7] and for extraction of geniposidic acid and aucubin from *Eucommia ulmoides* Oliver[8] and chlorogenic acid and flavonoids from haskap leaves (*Lonicera caerulea*).[9] TLPSs have been used for extraction and separation of liquiritin and glycyrrhizic acid from licorice (*Glycyrrhiza uralensis* Fisch)[10] and for simultaneous extraction of hydrophilic lithospermic acid B and lipophilic tanshinone IIA from *Salvia Miltiorrhiza* Bunge.[11] Compared to single-phase systems, ATPS demonstrates various advantages such as integrability, scalability, biocompatibility, selectivity, low interfacial tension, and continuous operation possibility.[3]

In extraction from biomass, the organic-salt-based ATPS was popular due to easy recycle of organics and salts, low viscosity, and easy phase separation. For ATPS based on organics and salts, there are a large number of possible combinations of phase-forming components to create ATPS. For the extraction of a specific target component, selection of ATPS components is generally carried out by an experimental trial and error method. Exhaustive and systematic experiments are required to guarantee the reliability and rationality of selection. Until now, the theoretical method for selection has not been found. With the wide application of ATPS extraction to more targets and more fields, it is necessary to replace some tedious and onerous experimental work with theoretical calculations, which is environment-friendly, time-saving, and cost-saving. In this paper, taking paeonol extraction as an example, we intended to explore the feasibility of the theoretical method for selection of ATPS. The theoretical results by calculation were evaluated with experiments, and the potential use for screening of ATPS in the extraction of small biomolecules was discussed.

Received: April 30, 2022
Accepted: August 11, 2022
Published: August 22, 2022

Paeonol with anti-bacterial and anti-tumor activities is a main active component in *cortex moutan*, which is the dry root bark of ranunculaceae peony. Effective extraction of paeonol from *cortex moutan* attracted attention due to its use as an active ingredient in paeonol ointment in China. In our previous work, the ATPS extraction of paeonol demonstrated advantages of high yield and high purity compared to single-phase extraction (70% ethanol).[12] However, large amounts of experiments were required to screen the organic solvent type and fraction and salt concentration. It is interesting to develop a green and sustainable theoretical calculation method to largely reduce the workload.

In extraction from herbs with ATPS, the mixture contains three phases, including two liquid phases and one solid phase (herb phase). At equilibrium, paeonol was mainly concentrated in the organic solvent-rich phase (top phase), but rarely distributed in the salt-rich phase (bottom phase), because paeonol was lipophilic with lg$P$ (PBS, pH 2, and P is the oil–water partition coefficient) 2.99.[13] Therefore, the extraction process could be roughly regarded as migration of paeonol from the herb phase to the top phase, and the organic-rich phase was determinant in the extraction process and equilibrium. The Gibbs free energy change (ΔE) for the extraction process can be expressed as eq 1.

$$\Delta E = E_{top} - E_{herb} \quad (1)$$

where E_{top} and E_{herb} represent the paeonol single-point energy in the top phase and in the herb phase, respectively. In all extraction cases, E_{herb} could be regarded as a constant, while in the top phase of different ATPS, E_{top} showed a difference. If E_{top} is low, the migration process is more spontaneous, and the partition coefficient between the top phase and the herb phase tends to increase, that is, the extraction yield tends to increase. Therefore, by comparing E_{top}, the ATPS with a low E_{top} energy was sorted out. For a convenient expression, the solvation free energy (E_{solv}) expressed in eq 2 was employed to compare the paeonol E_{top} values for each top phase of ATPS.

$$E_{solv} = |E_{top} - E_{gas}| \quad (2)$$

where E_{gas} is the single-point energy of paeonol at the gas state at 298 K. Generally, E_{top} is lower than E_{gas}, and so low E_{top} indicates high E_{solv}. E_{top} and E_{gas} could be calculated with Gaussian software.[14−16] The solvation model based on solute electron density (SMD) is one of the improved self-consistent reaction-field continuum solvation model in density function theory.[17] For example, the SMD model demonstrated good performance in correlation of solvation free energy with aqueous pK_a values.[18] In conclusion, the extraction yield had a relationship with solvation free energy. Therefore, the experimental extraction yield as an indicator in the optimization of ATPS compositions could be replaced with the theoretical solvation free energy.

The flowchart for the selection of solvent type, solvent fraction, and aqueous salt concentration in ATPS is illustrated in Figure 1.

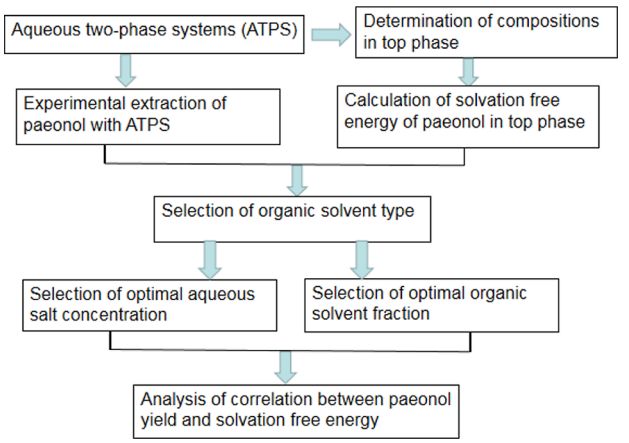

Figure 1. Flowchart for the optimization of solvent type, solvent fraction, and aqueous salt concentration in paeonol extraction.

EXPERIMENTAL SECTION

Reagents. *Cortex moutan* was purchased from Boren Pharmaceutical Co. Ltd. (Sichuan, China). The paeonol standard was from Yuanye Co. Ltd. (Nanjing, China). Concentrated hydrochloric acid, ethanol (EtOH), acetone, tetrahydrofuran (THF), and ethyl acetate (EA) of analytical grade were purchased from Kelong Chemical Co. Ltd. (Chengdu, China). NaOH was from Aladdin (Shanghai) Co. Ltd. $NaH_2PO_4{\cdot}2H_2O$ was bought from Sinopharm Group Chemical Reagent Co. Ltd. Methanol of chromatographical purity was from Shanghai Xingke Chemical Co. Ltd. Karl Fischer reagent was from Tansoole Co. Ltd. (Shanghai). The deionized water was used in the extraction and HPLC analysis.

Apparatus. The HPLC machine (LC4000) was from Jinpu Instrumental Co. Ltd. (Shandong, China). An SHA-C thermostat water bath oscillator for maintaining the temperature and oscillation in extraction was obtained from Aohua Instrument Co. Ltd. (Changzhou, China). The micro-moisture (WS-3) analyzer was from Zibo Zhenggong Instrument Factory (Shandong, China). The Gaussian 09 software package was used for the calculation. Linear regression was carried out with Software Origin 8.5 for the analysis of correlation between the extraction yield and the solvation free energy.

Methods. *Determination of Compositions in the Top Phase for ATPS and Calculation of Parameters for the Top-Phase Medium.* ATPS were formed by mixing an aqueous NaH_2PO_4 solution (pH 3.00) and an organic solvent (acetone, EtOH, THF, EtOH + EA or acetone + EA, or THF + EA) in a tube with a total volume of 25.00 mL. After keeping for 24.0 h at 25 °C, the top phase was separated with the bottom phase. Then, the compositions of the top phase were determined as follows. The mass of 2.00 mL top phase was recorded with a balance, and then, the volatiles were evaporated under vacuum to leave the solid of $NaH_2PO_4{\cdot}nH_2O$. In addition, after drying in an oven at 110 °C for 3.0 h, the weight of NaH_2PO_4 was acquired with a balance. The water content was determined by a micro-titration method with the Karl Fischer reagent using a micro-moisture (WS-3) analyzer. The organic solvent fraction was calculated by subtracting the water mass and salt mass from total mass. Due to big polarity difference between water and EA, there is even bigger polarity difference between EA and the bottom phase of ATPS because the bottom phase contained a salt of high concentration, which could salt-out "ethanol" to the top phase. EA with a dielectric coefficient of 5.99 shows far weaker polarity than ethanol with a dielectric coefficient of 24.85, and so it was reasonably assumed that the EA partitioned in the top phase, and its partition in the salt-rich phase was omitted. Then, the EtOH mass was calculated by subtracting the EA mass from the total organic solvent mass. The mass of each organic solvent (or an aqueous

https://doi.org/10.1021/acsomega.2c02693
ACS Omega 2022, 7, 30920−30929

NaH_2PO_4 solution) was divided by its density to give the volume. Finally, volume fractions for organic solvent or aqueous NaH_2PO_4 solution were calculated.

For the calculation of single-point energy, five parameters including static dielectric coefficient (ε_{esp}), dynamic dielectric coefficient (ε_{espinf}), hydrogen bond acidity (α), hydrogen bond basicity (β), and surface tension (γ) of the top-phase medium were considered. Each parameter was calculated with the model for a binary/ternary mixture using eq 3.[16,19,20]

$$y = bx_1 + cx_2 + dx_3 \quad (3)$$

where y is value for any of the parameters for the top phase mixture, b is the parameter value for the aqueous NaH_2PO_4 solution, c is the parameter value for EtOH/acetone/THF and d is the parameter value of EA, and x_1, x_2, and x_3 are the respective volume fractions of the aqueous NaH_2PO_4 solution, EtOH/acetone/THF, and EA in the top phase. The parameters for pure solvents (b, c, and d) are listed in Table S1, and an example for the calculation of parameter values is provided in the Supporting Information.

In eq 3, parameter b for an aqueous salt solution could not be obtained from the literature, and so, the parameters for water were employed. Each parameter value y calculated with eq 3 was not in line with the true value, and so, E_{solv} was not the true value. If the water content in the top phase was high, the salt content in the top phase was high, and if water content in the top phase was low, the salt content in the top phase was low. As is well known, a high salt concentration would escalate the dielectric coefficient in the top phase. High water content also escalates the dielectric coefficient because the dielectric coefficient of water is far higher than that of an organic solvent. In conclusion, both high salt content and high water content escalate the dielectric coefficient. The dielectric coefficient was a dominant parameter for single-point energy, signifying that both factors of salt content and water content resulted in the change of E_{solv} in the same trend. Therefore, the relative rank of E_{solv} did not vary even if the salt content was not considered in calculation. Based on the rank, the optimal ATPS would be selected.

Procedure for Calculation of Single-Point Energy of Paeonol. The paeonol structure was drawn with GaussView 5.0. With the hybrid functional B3LYP/6-31G* level,[21] its geometry structure was optimized, and the frequency was calculated using Gaussian 09 software.[14] The optimized structure is illustrated in Figure S1 in the Supporting Information. On the premise that there was no imaginary frequency, single-point energy for paeonol was calculated with the optimized structure at the M052X/6-31G* level.[22] The running language for the calculation of single-point energy is attached in the Supporting Information.

General Procedure for the Extraction of Paeonol with ATPS. The method and conditions such as pH, extraction period, and temperature were referred to our previous work.[12] The particle size for *cortex moutan* sieved through was less than 0.25 ± 0.058 mm. The total volume of ATPS was kept as 25.00 mL. ATPS was formed by adding an aqueous NaH_2PO_4 solution (pH 3.00) and an organic solvent (acetone, THF, EtOH, acetone + EA, THF + EA, or EtOH + EA) in a tube. Then, *cortex moutan* powder (0.500 ± 0.002 g) was added for extraction. Unless otherwise stated, after keeping at 25 °C for 12.0 h, the mixture was shaken at 37 °C for 8.0 h, the aqueous NaH_2PO_4 solution concentration was 3.85 mol/L and the total organic solvent fraction was 35.2%. After extraction, the herb fiber residue was removed by filtration. The top phase and the bottom phase were separated, and their volumes were recorded, respectively. The respective paeonol concentrations in the top phases were analyzed by HPLC with a method reported previously.[12]

The paeonol yield (Y, mg) was calculated using eq 4.

$$Y = C_T \cdot V_{Te} \quad (4)$$

where C_T (mg/mL) and V_{Te} (mL) represent the paeonol concentration in the top phase and the top-phase volume after extraction, respectively. The partition coefficient (K) and the phase ratio (β) were defined in eqs 5 and 6.

$$K = \frac{C_T}{C_B} \quad (5)$$

$$\beta = \frac{V_T}{V_B} \quad (6)$$

where C_B, V_T, and V_B are the paeonol concentration in the bottom phase, top-phase volume, and bottom-phase volume prior to extraction, respectively.

RESULTS AND DISCUSSION

Hypothesis and Design. The organic-rich phase was crucial for the extraction process and extraction equilibrium, and paeonol was mainly distributed in this phase. eq 1 is correct on the condition that the partition of paeonol in the bottom phase was too poor, and so paeonol solvation free energy in the bottom phase was not concerned. It should be noted that although the bottom phase was not determinant in the extraction equilibrium, it was important for extraction by softening the herb fiber and extracting out the hydrophilic compounds such as saccharides and proteins, which possibly deterred the penetration of a weakly polar solvent into the inner part of the herb particle. The paeonol E_{top} was the main factor for the paeonol yield. The presence of salt greatly affected the ε_{esp} of the top phase. Therefore, the calculated solvation free energy values were not the true values. However, in the various top phases of ATPS, the calculated E_{solv} values would be in the same rank as that for the true E_{solv} values because both the true E_{solv} and the calculated E_{solv} strongly dependent on the compositions in the top phase. Therefore, by comparing the rank of the calculated E_{solv}, ATPS components could be selected. After extraction, oil and inorganic salts from herbs were extracted and partitioned into ATPS, resulting in changes of the compositions in ATPS, and accordingly parameters for the top phase changed. This change was neglected in calculation.

For any parameter of a pure solvent (*e.g.*, ε_{eps}, ε_{epsinf}, α, β, and γ), different research groups usually reported different values. E_{solv} was slightly different from each other accordingly if the parameters were from different references. For all the pure solvents, ε_{eps} and ε_{epsinf} were from the Gaussian software;[14] α and β values were referred from the literature;[23] and the γ values were from the solvent handbook[24] to ensure the appropriate rank of the single-point energy.

Selection of Organic Solvent Type for ATPS in Paeonol Extraction. In consideration of paeonol lipophilicity,[13] six types of ATPS including EtOH−NaH_2PO_4−H_2O (ATPS-EtOH), EtOH-EA-NaH_2PO_4−H_2O (ATPS-EtOH-EA), acetone-NaH_2PO_4−H_2O (ATPS-acetone), acetone-EA-NaH_2PO_4−H_2O (ATPS-acetone-EA), THF-

https://doi.org/10.1021/acsomega.2c02693
ACS Omega 2022, 7, 30920−30929

NaH_2PO_4−H_2O (ATPS-THF), and THF-EA-NaH_2PO_4−H_2O (ATPS-THF-EA) were considered. Moreover, the organic solvents with low boiling points, low toxicity, and low viscosity are easily recycled and separated with paeonol by vacuum evaporation without altering the paeonol structure. The results are presented in Figure 2.

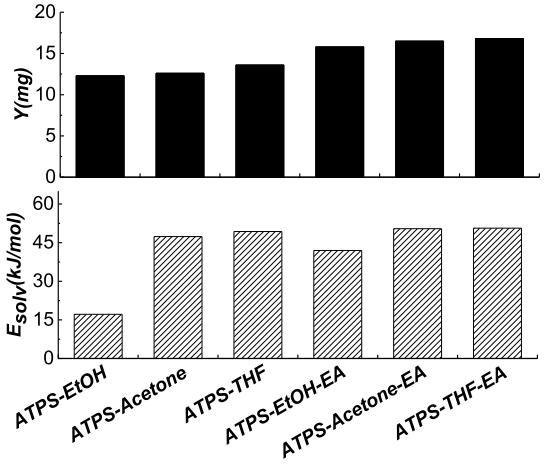

Figure 2. E_{solv} values and paeonol yields for the six types of ATPS. The total organic solvent fraction was kept as 35.2% for ATPS-EtOH, ATPS-EtOH-EA, ATPS-acetone, and ATPS-acetone-EA and as 30.4% for ATPS-THF and ATPS-THF-EA; aqueous NaH_2PO_4 concentration was 3.85 mol/L for ATPS-acetone and ATPS-acetone-EA, ATPS-THF, and ATPS-THF-EA and was 4.50 mol/L for ATPS-EtOH and ATPS-EtOH-EA; and EA fraction was 24.6, 24.6, and 10.6% in ATPS-EtOH-EA, ATPS-acetone-EA, and ATPS-THF-EA, respectively.

From Figure 2, it is clear that the paeonol E_{solv} values with ATPS were in the order ATPS-EtOH < ATPS-EtOH-EA < ATPS-acetone < ATPS-THF < ATPS-acetone-EA < ATPS-THF-EA. The E_{solv} values for ATPS-EtOH and ATPS-EtOH-EA were far lower than the other E_{solv} values of four ATPS.

The experimental yields with the above six ATPS were in the order ATPS-EtOH < ATPS-acetone < ATPS-THF < ATPS-EtOH-EA < ATPS-acetone-EA ≈ ATPS-THF-EA. Except for ATPS-EtOH-EA, with the other five ATPS, the paeonol E_{solv} was in the same order as the experimental yield. Possibly, it was resulted from other minor factors in extraction, and they will be discussed in the following section.

Selection of Optimal Organic Solvent Fraction in ATPS-Acetone and ATPS-THF for Extraction. The compositions, parameter values, and E_{solv} for ATPS-acetone and ATPS-THF with various organic fractions are listed in Table S2. The E_{solv} and paeonol yield as a function of organic solvent fraction in ATPS are presented in Figure 3. The organic solvent fraction in the range 25.6−40.0% was employed due to the following reasons. If the organic fraction was too low, the volume of the top phase was too small, and the top-phase loss would be relatively high during the processes such as filtration and transfer, resulting in high target loss or poor yield. If the fraction of organic solvent is too high, some of the target molecules distributed in the bottom phase, resulting in poor yield. Moreover, the organic solvent is generally expensive, and so high fraction of organic solvent is generally avoided.

As shown in Figure 3a, in paeonol extraction with ATPS-acetone, both E_{solv} and paeonol yield ascended as the acetone fraction increased from 25.6 to 35.2%, but when the acetone fraction was above 35.2%, both paeonol E_{solv} and paeonol yield declined. It suggested that the two curves for the paeonol yield and the E_{solv} as a function of the acetone fraction demonstrated a similar trend. Both E_{solv} and yield attained a peak value at an acetone fraction of 35.2%.

With the increase of the acetone fraction from 25.6 to 35.2%, in the top phase, the organic solvent fraction increased and the water fraction decreased, and accordingly, ε_{eps} and α decreased, while β increased. The decrease of the ε_{eps} suggested the enhancement of hydrophobicity interaction between paeonol and the top-phase medium. There are two types of hydrogen bond interactions between paeonol and the top-phase medium. A type-1 hydrogen bond is formed between the hydrogen of the top-phase medium (from water or ethanol) and the oxygen in paeonol, and a type-2 hydrogen bond is formed between the oxygen of the top-phase medium and the hydrogen of the hydroxyl group in paeonol. As the acetone fraction increases, the decrease of α in the top-phase medium indicated weakening of the type-1 hydrogen bond interaction, and the increase of β indicated the enhancement of the type-2 hydrogen bond interaction. The overall effect rendered E_{solv} increase as the acetone fraction increases from 25.6 to 35.2%. However, with the increase of acetone fraction from 35.2 to 37.6%, the phase ratio increased from 0.900 to 1.00, the acetone fraction in the top-phase decreased slightly

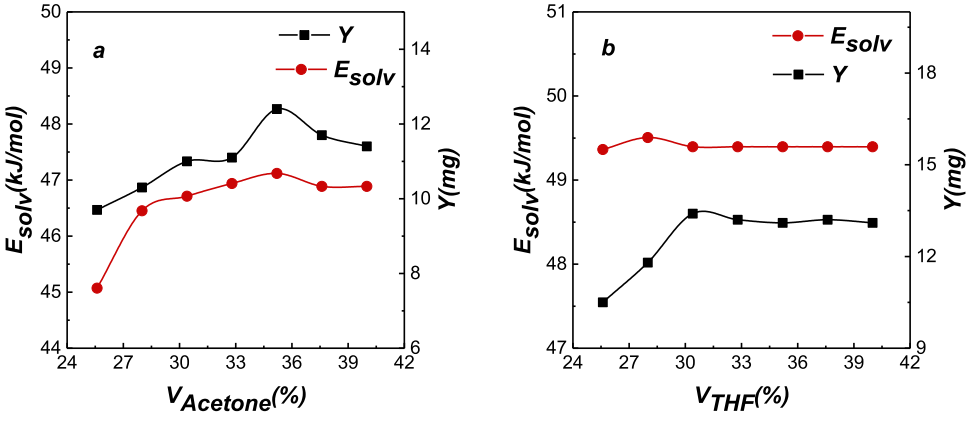

Figure 3. Paeonol yield and solvation free energy as a function of organic fraction for (a) ATPS-acetone and (b) ATPS-THF. The aqueous $Na_2H_2PO_4$ concentration was 3.85 mol/L.

https://doi.org/10.1021/acsomega.2c02693
ACS Omega 2022, 7, 30920−30929

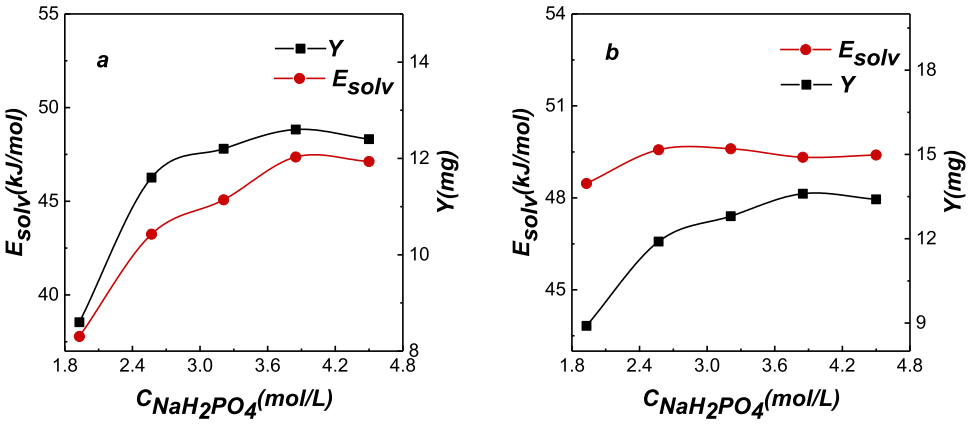

Figure 4. Paeonol yield and solvation free energy as a function of aqueous NaH_2PO_4 concentration for ATPS: (a) acetone-NaH_2PO_4−H_2O and (b) THF-NaH_2PO_4−H_2O. The volume fractions for acetone and THF were 35.2 and 30.4%, respectively.

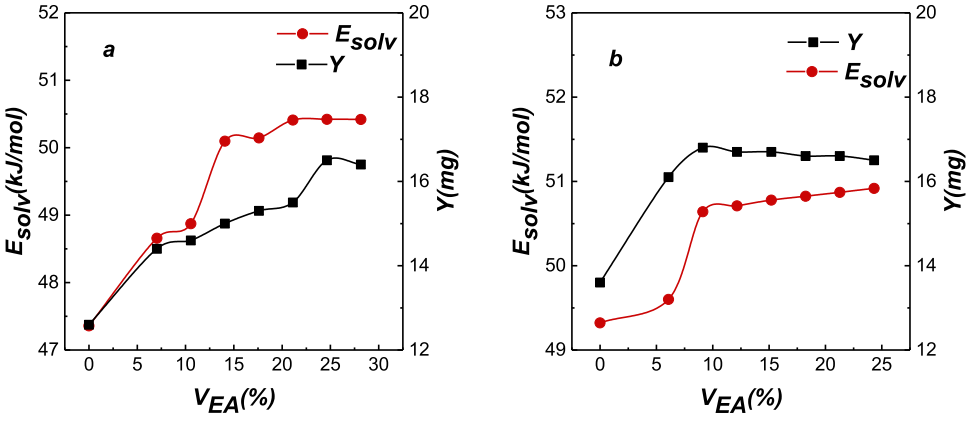

Figure 5. E_{solv} and paeonol yield against the EA volume fraction in paeonol extraction with (a) ATPS-acetone-EA and (b) ATPS-THF-EA. For ATPS-acetone-EA and ATPS-THF-EA, the total organic fractions were set as 35.2 and 30.4%, respectively.

from 61.31 to 61.02%, and accordingly, the E_{solv} value slightly decreased. When the acetone fraction increases from 37.6 to 40.0%, the phase ratio increased from 1.00 to 1.14, the organic solvent fraction in the top phase changed inappreciably, and so the E_{solv} value did not alter significantly.

From Figure 3a, it can be concluded that the plot of E_{solv} as a function of acetone fraction demonstrated a similar trend to the plot of the experimental yield, and E_{solv} values successfully predict the optimal acetone fraction. It suggested that for ATPS-acetone, the theoretical paeonol E_{solv} rank could work in selecting the optimal acetone fraction in paeonol extraction.

Figure 3b shows the plots of E_{solv} and paeonol yield against THF fraction in ATPS-THF. With the increase of THF fraction in ATPS from 25.6 to 28.0%, the THF fraction in the top phase ascended slightly from 61.9 to 62.1%, ε_{eps} declined, and thus E_{solv} increased slightly. However, E_{solv} declined slightly with the increase of the THF fraction from 28.0 to 30.4% due to the decrease of THF content to 62.0%. With the THF fraction over 30.4%, E_{solv} did not change due to the consistency of compositions. By comparing the rank of the E_{solv}, the optimal THF fraction was 28.0%. However, Figure 3b shows that the yield achieved a peak value with a THF fraction of 30.4%. A slightly higher experimental yield with a THF fraction of 30.4% than that of 28.0% was possibly the result of a higher phase ratio (0.45 against 0.38) and a higher partition coefficient (44.0 against 38.5).

In conclusion, for ATPS-acetone and ATPS-THF, the theoretical E_{solv} could be employed for the selection of solvent fraction.

Selection of Aqueous NaH_2PO_4 Concentration for ATPS in Paeonol Extraction. The salt concentration affected the compositions of the top phase and thus affected the extraction yield. The salt effect on paeonol E_{solv} was greatly concerned.

The top-phase compositions, parameters, and E_{solv} for ATPS-acetone and ATPS-THF with various aqueous NaH_2PO_4 concentrations are listed in Table S3. E_{solv} and the experimental yield against the aqueous NaH_2PO_4 concentration for ATPS-acetone and ATPS-THF are presented in Figure 4a,b, respectively.

From Table S3, it is clear that as the aqueous NaH_2PO_4 concentration increases to 3.85 mol/L, the acetone fraction increased, but the water content decreased in the top phase, and so ε_{eps}, α, and γ decreased, but β increased. It indicated that the hydrophobicity interaction between paeonol and the top-phase medium enhanced, and the hydrogen bond interaction of type-1 decreased, but the hydrogen bond interaction of type-2 increased. As a result, both E_{solv} and the experimental yield were improved with the increase of the salt concentration. When the aqueous NaH_2PO_4 concentration was below 2.35 mol/L, both the curves in Figure 4a demonstrated a sharp slope; while the salt concentration was from 2.35 to 3.85 mol/L, the slope became even. However, with the

https://doi.org/10.1021/acsomega.2c02693
ACS Omega 2022, 7, 30920−30929

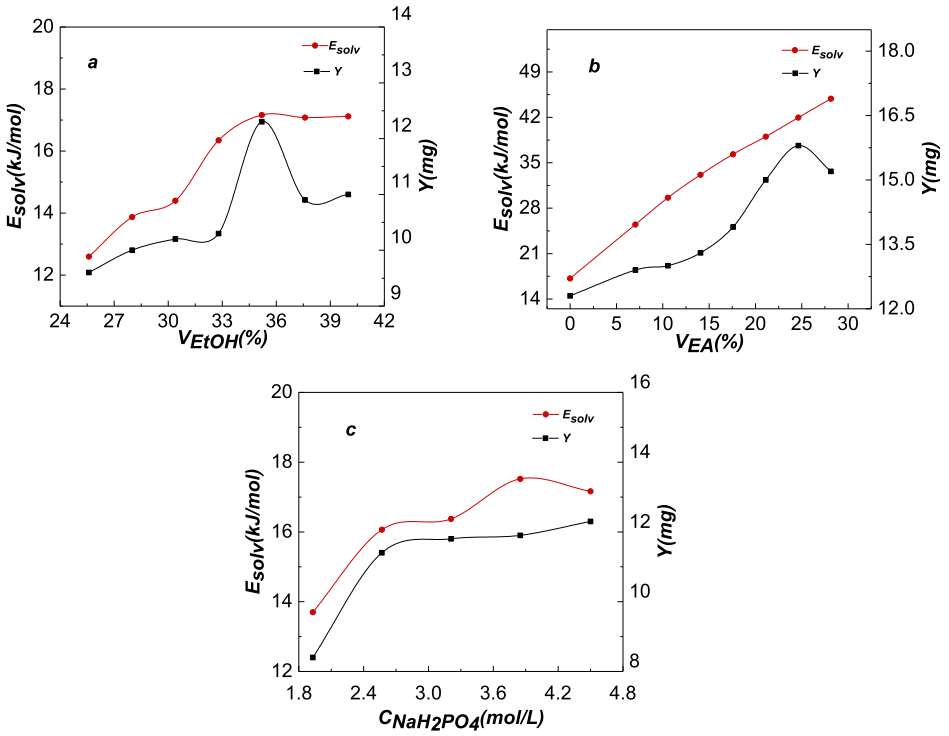

Figure 6. Solvation free energy and paeonol yield for ATPS-EtOH and ATPS-EtOH-EA against (a) ethanol fraction; (b) EA fraction; and (c) aqueous NaH_2PO_4 concentration. The total organic fraction was set as 35.2% for ATPS-EtOH-EA.

increase of the aqueous NaH_2PO_4 concentration from 3.85 to 4.50 mol/L, the phase ratio decreased from 1.14 to 0.910, and in the top phase, the acetone content decreased from 61.55 to 61.35%. Accordingly, both the yield and E_{solv} descended slightly. In conclusion, the curve for E_{solv} demonstrated a similar trend to that for the experimental yield. Both the curves for yield and E_{solv} indicated that the optimal aqueous NaH_2PO_4 concentration was 3.85 mol/L. A good coincidence for the two curve trends in Figure 4a suggested that the theoretical E_{solv} was a reliable parameter in salt concentration optimization.

For ATPS-THF in Table S3, as the aqueous NaH_2PO_4 concentration increases to 3.21 mol/L, in the top phase, the THF fraction increased, but the water content decreased, resulting in a decrease of ε_{eps}, α, and γ but an increase of β. Like the case in ATPS-acetone, both E_{solv} and the yield were improved with the increase of the salt concentration to 3.21 mol/L.

Figure 4b shows that, although the curve trend for E_{solv} did not demonstrate a perfect coincidence with that for the paeonol yield, the change was insignificant with the increase of the salt concentration from 3.21 to 3.85 mol/L. From the above discussion, it showed that the theoretical E_{solv} could work for selecting an optimal salt concentration.

By the aforementioned discussion, low ε_{eps} generally demonstrated high E_{solv}. Therefore, we inferred that addition of ethyl acetate with lower ε_{eps} would improve E_{solv} and the extraction yield. It was interesting to clarify if the optimal fraction of EA could be chosen by using E_{solv} as an indicator.

Ethyl Acetate Fraction in ATPS-EA for Paeonol Extraction. The compositions, parameter values, and E_{solv} for ATPS-acetone-EA and ATPS-THF-EA with different EA fractions are presented in Table S4. The paeonol E_{solv} and experimental yield for ATPS-acetone-EA and ATPS-THF-EA as a function of EA fraction are presented in Figure 5a,b, respectively.

For ATPS-acetone-EA in Table S4, as the EA fraction increases from 0 to 24.6%, ε_{eps} and α decreased, suggesting that the hydrophobicity interaction between "paeonol and top phase medium" strengthened, but the decrease of α indicated that the hydrogen bond interaction of type-1 weakened. The hydrogen bond basicity decreased with the EA fraction from 0 to 10.6% and from 14.1 to 28.2% but increased slightly with the EA fraction from 10.6 to 14.1%. As shown in Figure 5a, the decrease of ε_{eps} rendered E_{solv} escalate sharply with the increase of the EA fraction from 0 to 14.1%, and E_{solv} improved in a small step until the EA fraction attained 24.6%. When the EA fraction was from 24.6 to 28.2%, E_{solv} increased insignificantly. E_{solv} suggested that the optimal EA fraction was 24.6% or 28.2%.

As shown in Figure 5a, the experimental yield improved as the EA fraction increases to 24.6%. When the EA fraction was over 24.6%, the paeonol yield declined appreciably. During the experiments, we observed that with an EA fraction of 28.2%, a small amount of solvent was soaked into herb, suggesting a poor penetration of the top-phase medium into the herb. Therefore, the paeonol dissolution rate became slow, and possibly, the extraction did not attain equilibrium at 8 h. Poor penetration of the top-phase medium with too high EA fraction could be shadowed by the declines of α and β values in Table S4. The herb fiber mainly contains saccharides, amino acids, and proteins having hydroxyl groups and amide groups, which can form a hydrogen bond with a liquid medium of good α and β values. The interactions "between herb fiber and solvent" really affected the experimental yield, but they did not influence E_{solv}. The experimental yield demonstrated that the optimal EA fraction was 24.6%. It suggested that E_{solv} as an indicator could really reduce the experimental workload.

https://doi.org/10.1021/acsomega.2c02693
ACS Omega 2022, 7, 30920−30929

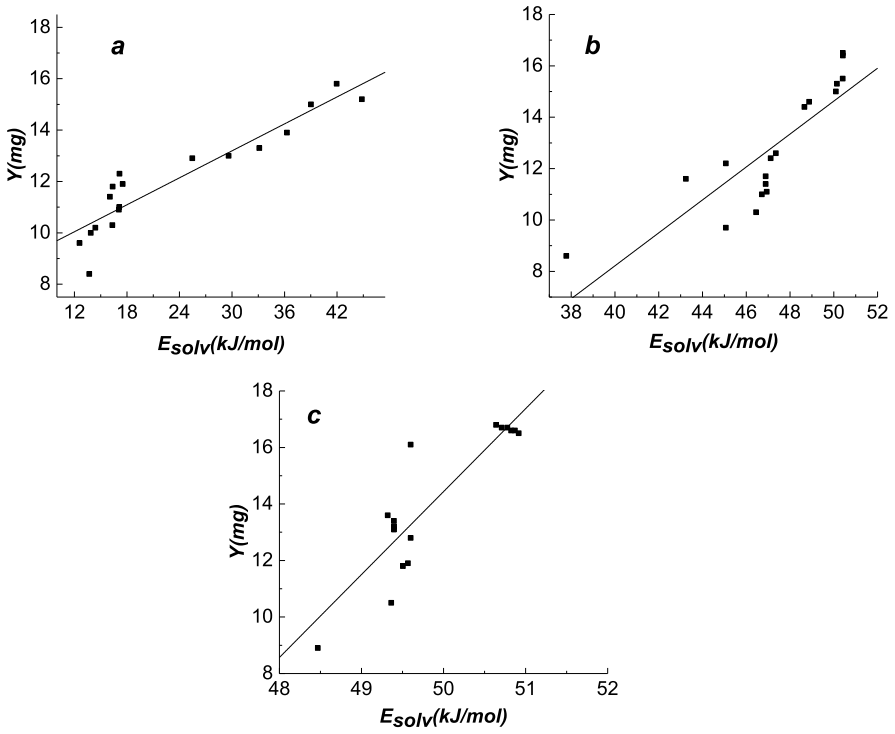

Figure 7. Analysis of linear correlation between E_{solv} and the paeonol yield for (a) ATPS-EtOH and ATPS-EtOH-EA [$Y = 0.175\ E_{solv} + 7.94$ ($R^2 = 0.8555$, $n = 18$)]; (b) ATPS-acetone and ATPS-acetone-EA [$Y = 0.641\ E_{solv} - 17.4$ ($R^2 = 0.7027$, $n = 18$)]; and (c) ATPS-THF and ATPS-THF-EA [$Y = 2.93\ E_{solv} - 132.3$ ($R^2 = 0.7816$, $n = 18$)].

In Table S4 for ATPS-THF-EA, as the EA fraction increases to 9.12%, ε_{eps} decreased, suggesting that the hydrophobicity interaction between paeonol and the top-phase medium strengthened, and both the α and β values decreased, suggesting that both types of hydrogen bond interactions weakened. However, as the EA fraction increases from 9.12 to 24.3%, E_{solv} increased slightly.

Figure 5b shows that for ATPS-THF-EA, the experimental yield ascended as the EA fraction increases to 9.12% but descended very slightly when the EA fraction increased from 9.12 to 24.3%. Like the case for ATPS-acetone-EA, when the EA fraction was over 9.12%, a decrease of β and ε_{esp} possibly retarded the penetration of the top-phase medium into the herb phase and also weakened the hydrogen bond interactions between paeonol and the top-phase medium. Although the best EA fraction with ATPS-THF-EA was not predicted by E_{solv} accurately, in Figure 5b, both E_{solv} and the experimental yield altered in a very small range when the EA fraction was over 9.12%, and E_{solv} could roughly point out the turning point of EA fraction and could narrow the experimental range for EA fraction.

In conclusion, E_{solv} demonstrated good performance to select the organic solvent fractions in ATPS-acetone, ATPS-THF, ATPS-acetone-EA, and ATPS-THF-EA and the aqueous NaH_2PO_4 concentration in ATPS-acetone and ATPS-THF. To see whether or not the theoretical E_{solv} could be used for the selection of optimal organic solvent fraction and aqueous salt concentration in other ATPS, E_{solv} and the experimental yield with ATPS-EtOH and ATPS-EtOH-EA were investigated.

Solvation Free Energy and Paeonol Yield in Extraction with ATPS-EtOH and ATPS-EtOH-EA. For ATPS-EtOH and ATPS-EtOH-EA, the experimental yield and E_{solv} against EtOH fraction, EA fraction, and aqueous NaH_2PO_4 concentration are presented in Figure 6a–c, respectively.

Selection of Optimal Ethanol Fraction in ATPS-EtOH. The compositions, parameter values, and E_{solv} for ATPS-EtOH with various ethanol fractions are presented in Table S5. As the ethanol fraction increases from 25.6 to 35.2%, the ethanol content in the top phase increased, resulting in a decrease of ε_{esp}, α, and γ but an increase of β. It suggested that the hydrophobicity interaction between paeonol and the top-phase medium enhanced; the hydrogen bond interaction of type-1 decreased, but the hydrogen bond interaction of type-2 strengthened. In total, E_{solv} increased. However, when the ethanol fraction was from 35.2 to 40.0%, as the phase ratio increased sharply from 1.14 to 1.86, the ethanol content did not increase any more. ε_{esp}, α, and β changed insignificantly. Therefore, E_{solv} did not change obviously. From Figure 6a, it can be observed that as the ethanol fraction increases from 25.6 to 35.2%, both E_{solv} and the experimental yield increased. With the ethanol fraction above 35.2%, E_{solv} altered insignificantly, but the paeonol yield decreased slightly, possibly because of the decrease of partition coefficient, resulting in loss of paeonol in the bottom phase in experiments. Both curves demonstrated that the optimal ethanol volume fraction was 35.2%, suggesting that the theoretical calculation method was feasible to choose an optimal ethanol fraction.

Selection of Optimal EA Fraction in ATPS-EtOH-EA. For ATPS-EtOH-EA with different EA fractions, the compositions, parameters, and E_{solv} are presented in Table S6. As shown in Table S6, addition of EA in ATPS rendered the top phase to contain more fraction of organics but lower fraction of water. Together with the low ε_{esp} of EA, ε_{eps} decreased markedly, indicating that the hydrophobicity interaction between paeonol and the top-phase medium enforced, and α and β decreased, suggesting that the hydrogen bond interactions of both type-1

https://doi.org/10.1021/acsomega.2c02693
ACS Omega 2022, 7, 30920−30929

and type-2 weakened. In total, E_{solv} increased as the EA fraction increases.

Figure 6b shows that the experimental yield escalated as the EA fraction increases until the fraction attained 24.6%. When the EA fraction was over 24.6%, the yield decreased. Presumably, with an EA fraction of 28.2%, the hydrogen bond interactions between the top-phase medium and the herb fiber descended, resulting in a poor solvent penetration into the herb. Moreover, high hydrophobicity of the top-phase medium also prevented the penetration of solvents into the herb fiber. Also, with the increase of the EA fraction to 28.2%, the phase ratio decreased to 0.6, and a small volume of the top phase resulted in a relatively high paeonol loss during filtration and transfer processes. In spite of the imperfect prediction of the optimal EA fraction, E_{solv} could offer guidance for optimization experiments.

Selection of Optimal Aqueous NaH_2PO_4 Concentration in ATPS-EtOH. For ATPS-EtOH with different aqueous NaH_2PO_4 concentrations, the compositions, parameters, and E_{solv} are presented in Table S7. With the increase of the aqueous NaH_2PO_4 concentration, the "salting out" effect enforced, and therefore, in the top phase, the ethanol content increased, resulting in a decrease of ε_{esp} and α but an increase of β. It suggested that the hydrophobicity interaction between paeonol and the top-phase medium enhanced, the type-1 hydrogen bond interaction decreased, but the hydrogen bond interaction of type-2 increased. In total, E_{solv} increased as the aqueous NaH_2PO_4 concentration increases to 3.85 mol/L, as shown in Figure 6c. With an aqueous NaH_2PO_4 concentration of 4.50 mol/L, the salt precipitated from ATPS during standing at 25 °C, and the true concentration in ATPS was below 4.50 mol/L. Therefore, in Table S7, it is shown that the EtOH content decreased but the water content in the top phase increased, resulting in an increase of ε_{eps}. Accordingly, E_{solv} declined. However, the extraction experiments were carried out at 37 °C, the salt did not precipitate from ATPS at a NaH_2PO_4 concentration of 4.50 mol/L, and so the yield was higher than that with a salt concentration of 3.85 mol/L. Moreover, with high salt concentration, the partition coefficient improved, and the experimental yield improved slightly. It was clear that E_{solv} and the yield increased sharply with the increase of the aqueous NaH_2PO_4 concentration from 2.35 to 2.93 mol/L; and both E_{solv} and the yield increased insignificantly from 2.93 to 3.85 mol/L, that is, both curves in Figure 6c exhibited a similar trend. The inconsistency of the two curves with the concentration range of 3.85−4.50 mol/L possibly resulted from the salt precipitation in ATPS for the determination of top-phase compositions.

Analysis of Correlation between Solvation Free Energy and Experimental Yield. For ATPS-EtOH, ATPS-EtOH-EA, ATPS-acetone, ATPS-acetone-EA, ATPS-THF, and ATPS-THF-EA systems, the paeonol free energy E_{solv} demonstrated a correlation with paeonol yield. Therefore, we intended to establish a mathematical model to describe the correlation. With each series of 18 ATPS, the experimental yield was plotted against E_{solv} to give Figure 7a−c for a group of ATPS-EtOH plus ATPS-EtOH-EA, a group of ATPS-acetone plus ATPS-acetone-EA, and a group of ATPS-THF plus ATPS-THF-EA, respectively.

For each series of ATPS, the correlation coefficients suggested that the experimental yield had a relationship with E_{solv}. However, with all the 54 ATPS, the paeonol yield had a poor linear relationship with E_{solv}. The poor correlation coefficient could be seen by the inconsistent intercepts and slope of the curves shown in Figure 7. The possible reasons for the above problem were due to some factors resulting in inconsistency of the theoretical calculation and experimental yield. E_{solv} is a dominant factor but not a sole factor for the experimental yield. The extraction process includes multisteps of extraction, filtration, transfer, and determination of sample, and experimental yield was affected by lots of other factors. (1) Only the interaction between paeonol and the top-phase medium was considered in theoretical calculations, but in experiments, there were other factors. In many cases, the penetration ability of the solvent medium might not affect the extraction, but in some cases, the top phase solvent with very low ε_{eps}, low hydrogen bond acidity, and low hydrogen bond basicity demonstrated poor penetration ability. This can be seen in the extraction with ATPS containing EA. (2) The phase ratio was also a factor on the experimental yield. Although E_{sovl} with the unit kJ/mol had no relation with phase ratio, during the experiments, the low phase ratio indicated a small volume of the top phase, resulting in a relatively high paeonol loss in the filtration and transfer processes. (3) For ATPS with a relatively high E_{solv}, paeonol might be extracted completely, but for other ATPS with even higher E_{solv} than a critical value, paeonol could not be improved further. For example, the yields for ATPS-acetone-EA and ATPS-THF-EA at optimal conditions showed a similar level, although their E_{solv} showed a significant difference. (4) The parameters for single-point energy calculation were obtained using linear approximation according to the compositions of the top phase and the parameters of a pure solvent rather than by direct determination. The parameter approximation possibly gave rise to the error for the E_{solv} rank in some cases. (5) In the calculation of theoretical E_{solv}, the temperature is set as 25 °C by Gaussian software and could not be set manually, but the experimental temperature was set as 37 °C to achieve quick extraction and good partition coefficient. Due to the above reasons, the correlation coefficient for each group of ATPS extraction was not so good compared to those for the linear correlation between the calculated and experimental pK_a values for thiols[25] or for the linear correlation between the calculated and experimental values for solvation free energies of 40 compounds in methanol.[20]

Although with all the ATPS the experimental yield demonstrated a poor linear relationship with the theoretical E_{solv}, with each series of ATPS, the linearity was reasonably good. Therefore, the paeonol yield could not be accurately predicted with E_{solv}, but the E_{solv} rank could be employed as a tool for the selection of optimal organic solvent type, solvent fraction, and aqueous salt concentration in ATPS.

CONCLUSIONS

Based on the hypothesis that paeonol was extracted from the herb phase to the liquid phase mainly by the route of top phase, the top-phase properties were dominant factors for extraction. The solvation free energy of paeonol in the top phase of 54 ATPS, which were classified into 3 groups, was calculated by Gaussian. It is feasible to use the E_{solv} rank for selecting the optimal organic solvent type and fraction and the aqueous salt concentration in ATPS extraction of paeonol. With each group of ATPS (18 × 3), the paeonol yield was correlated with the solvation free energy. Generally, high E_{solv} of paeonol in the top phase offered a good yield. For ATPS extraction of active components from the herb, by theoretical

https://doi.org/10.1021/acsomega.2c02693
ACS Omega 2022, 7, 30920−30929

optimization with E_{solv}, at least optimization experiments could be confined to a small range to save carbon fingerprint and cost. However, with all the 54 ATPS, the paeonol yield showed a poor linear correlation with solvation free energy due to the factors discussed in the above section. Hence, in future, the mathematical model will be calibrated to improve the prediction ability by consideration of the other minor factors.

■ ASSOCIATED CONTENT

Supporting Information

The Supporting Information is available free of charge at https://pubs.acs.org/doi/10.1021/acsomega.2c02693.

Parameters for pure solvents, calculation of parameters for the top phase in ATPS-EtOH and in ATPS-EtOH-EA, and running language for the calculation of single-point energy; parameter values and E_{solv} for various ATPS-acetone and ATPS-THF with different organic volume fractions; parameter values and E_{solv} for various ATPS-acetone and ATPS-THF with different NaH_2PO_4 concentrations; parameter values and E_{solv} for various ATPS-acetone and ATPS-THF with different EA fractions; parameter values and E_{solv} for various ATPS-EtOH with different EtOH fractions; parameter values and E_{solv} for various ATPS-EtOH with different EA fractions; and parameter values and E_{solv} for various ATPS-EtOH with different aqueous NaH_2PO_4 concentrations (PDF)

■ AUTHOR INFORMATION

Corresponding Author

Xiaojing Mu − *Department of Pharmaceutical Engineering, College of Chemistry & Chemical Engineering, Chongqing University, Chongqing 401331, China;* orcid.org/0000-0002-4929-6362; Phone: +8615923356992; Email: muxj@cqu.edu.cn

Authors

Haiming Huang − *Department of Pharmaceutical Engineering, College of Chemistry & Chemical Engineering, Chongqing University, Chongqing 401331, China*

Jing Deng − *Department of Pharmaceutical Engineering, College of Chemistry & Chemical Engineering, Chongqing University, Chongqing 401331, China*

Shangyou Xiao − *Department of Pharmaceutical Engineering, College of Chemistry & Chemical Engineering, Chongqing University, Chongqing 401331, China*

Zhiwei Luo − *Department of Pharmaceutical Engineering, College of Chemistry & Chemical Engineering, Chongqing University, Chongqing 401331, China*

Gang Chen − *Department of Pharmaceutical Engineering, College of Chemistry & Chemical Engineering, Chongqing University, Chongqing 401331, China*

Complete contact information is available at: https://pubs.acs.org/10.1021/acsomega.2c02693

Author Contributions

The manuscript was written through the contributions of all authors.

Notes

The authors declare no competing financial interest.

■ ACKNOWLEDGMENTS

This work was financially funded by the Commission of Science and Technology of Chongqing China for "Key generic technologies in key industries" (no cstc2016zdcy-ztzx10001). Also, thanks should be given to prof. Gang Feng in the Chemistry Department of Chongqing University for his kind help in running Gaussian software and beneficial discussion.

■ ABBREVIATIONS

ATPS	aqueous two-phase system(s)
ATPS-EtOH	ATPS based on ethanol, EtOH−NaH_2PO_4−H_2O
ATPS-acetone	ATPS based on acetone, acetone-NaH_2PO_4−H_2O
ATPS-THF	ATPS based on tetrahydrofuran, THF-NaH_2PO_4−H_2O
ATPS-EtOH-EA	ATPS based on ethanol plus EA, EtOH-EA-NaH_2PO_4−H_2O
ATPS-acetone-EA	ATPS based on acetone plus EA, acetone-EA-NaH_2PO_4−H_2O
ATPS-THF-EA	ATPS based on THF plus EA, THF-EA-NaH_2PO_4−H_2O
DFT	density functional theory
EA	ethyl acetate
EtOH	ethanol
SMD	solvation model based on solute electron density
THF	tetrahydrofuran
TLPS	three-liquid-phase system
ε_{esp}	static dielectric coefficient
ε_{espinf}	dynamic dielectric coefficient
α	hydrogen bond acidity
β	hydrogen bond basicity
γ	surface tension

■ REFERENCES

(1) Rosinha Grundtvig, I. P. R.; Heintz, S.; Krühne, U.; Gernaey, K. V.; Adlercreutz, P.; Hayler, J. D.; Wells, A. S.; Woodley, J. M. Screening of Organic Solvents for Bioprocesses Using Aqueous-organic Two-phase Systems. *Biotechnol. Adv.* **2018**, *36*, 1801−1814.

(2) dos Santos, N. V.; de Carvalho Santos-Ebinuma, V. D.; Pessoa, A., Jr.; Pereira, J. F. B. Liquid-liquid Extraction of Biopharmaceuticals from Fermented Broth: Trends and Future Prospects. *J. Chem. Technol. Biotechnol.* **2018**, *93*, 1845−1863.

(3) Pereira, J. F. B.; Freire, M. G.; Coutinho, J. A. P. Aqueous Two-phase Systems: Towards Novel and More Disruptive Applications. *Fluid Phase Equil.* **2020**, *505*, 112341.

(4) Torres-Acosta, M. A.; Mayolo-Deloisa, K.; González-Valdez, J.; Rito-Palomares, M. Aqueous Two-phase Systems at Large Scale: Challenges and Opportunities. *Biotechnol. J.* **2019**, *14*, 1800117.

(5) Zaslavsky, B. Y.; Uversky, V. N.; Chait, A. Analytical Applications of Partitioning in Aqueous Two-phase Systems: Exploring Protein Structural Changes and Protein−Partner Interactions in Vitro and in Vivo by Solvent Interaction Analysis Method. *Biochim. Biophys. Acta, Proteins Proteomics* **2016**, *1864*, 622−644.

(6) Vicente, F. A.; Bairos, J.; Roque, M.; Coutinho, J. A. P.; Ventura, S. P. M.; Freire, M. G. Use of Ionic Liquids as Cosurfactants in Mixed Aqueous Micellar Two-Phase Systems to Improve the Simultaneous Separation of Immunoglobulin G and Human Serum Albumin from Expired Human Plasma. *ACS Sustainable Chem. Eng.* **2019**, *7*, 15102−15113.

(7) Ruiz, C. A. S.; Kwaijtaal, J.; Peinado, O. C.; van den Berg, C.; Wijffels, R. H.; Eppink, M. H. M. Multistep Fractionation of Microalgal Biomolecules Using Selective Aqueous Two-Phase Systems. *ACS Sustainable Chem. Eng.* **2020**, *8*, 2441−2452.

https://doi.org/10.1021/acsomega.2c02693
ACS Omega 2022, 7, 30920−30929

(8) Wang, Y. C.; Wang, S. S.; Liu, L. L. Extraction of Geniposidic Acid and Aucubin Employing Aqueous Two-phase Systems Comprising Ionic Liquids and Salts. *Microchem. J.* **2021**, *169*, 106592.
(9) Chong, K. Y.; Stefanova, R.; Zhang, J. Z.; Brooks, M. S. L. Aqueous Two-phase Extraction of Bioactive Compounds from Haskap Leaves (Lonicera caerulea): Comparison of Salt/Ethanol and Sugar/Propanol Systems. *Sep. Purif. Technol.* **2020**, *252*, 117399.
(10) Wang, L. Q.; Chen, X. Y.; Liu, J. J.; Tan, Z. J. A LCST-type Ionic Liquid Used as the Recyclable Extractant for the Extraction and Separation of Liquiritin and Glycyrrhizic Acid from Licorice (Glycyrrhiza Uralensis Fisch). *J. Mol. Liq.* **2021**, *340*, 117295.
(11) Gou, Y.; Mu, X. J.; Li, Y.; Tang, M. L.; Chen, G.; Xiao, S. Y. Three-liquid-phase Extraction and Re-partition as an Integrated Process for Simultaneous Extraction and Separation of Lithospermic Acid B and Tanshinone IIA. *Biochem. Eng. J.* **2021**, *176*, 108173.
(12) Yi, X. Q.; Mu, X. J.; Chen, G.; Gou, Y.; Wang, C. S.; Yuan, X. L. Water-Insoluble Cosolvent in Aqueous Two-phase System Improved the Extraction of Paeonol from Cortex Moutan. *J. Chem. Technol. Biotechnol.* **2019**, *94*, 2229−2237.
(13) Zong, S. Y.; Pu, Y. Q.; Xu, B. L.; Zhang, T.; Wang, B. Study on the Physicochemical Properties and Anti-inflammatory Effects of Paeonol in Rats with TNBS-induced Ulcerative Colitis. *Int. Immunopharmacol.* **2017**, *42*, 32−38.
(14) Frisch, M. J.; Trucks, G. W.; Schlegel, H. B.; Scuseria, G. E.; Robb, M. A.; Cheeseman, J. R.; Scalmani, G.; Barone, V.; Mennucci, B.; Petersson, G. A.; Nakatsuji, H.; Caricato, M.; Li, X.; Hratchian, H. P.; Izmaylov, A. F.; Bloino, J.; Zheng, G.; Sonnenberg, J. L.; Hada, M.; Ehara, M.; Toyota, K.; Fukuda, R.; Hasegawa, J.; Ishida, M.; Nakajima, T.; Honda, Y.; Kitao, O.; Nakai, H.; Vreven, T.; Montgomery, J. A.; Peralta, J. E., Jr.; Ogliaro, F.; Bearpark, M.; Heyd, J. J.; Brothers, E.; Kudin, K. N.; Staroverov, V. N.; Kobayashi, R.; Normand, J.; Raghavachari, K.; Rendell, A.; Burant, J. C.; Iyengar, S. S.; Tomasi, J.; Cossi, M.; Rega, N.; Millam, J. M.; Klene, M.; Knox, J. E.; Cross, J. B.; Bakken, V.; Adamo, C.; Jaramillo, J.; Gomperts, R.; Stratmann, R. E.; Yazyev, O.; Austin, A. J.; Cammi, R.; Pomelli, C.; Ochterski, J. W.; Martin, R. L.; Morokuma, K.; Zakrzewski, V. G.; Voth, G. A.; Salvador, P.; Dannenberg, J. J.; Dapprich, S.; Daniels, A. D.; Farkas, O.; Foresman, J. B.; Ortiz, J. V.; Cioslowski, J.; Fox, D. J. *Gaussian 09, Revision A.1*; Gaussian, Inc.: Wallingford C.T, 2009.
(15) Guan, D.; Lui, R.; Matthews, S. LogP Prediction Performance with the SMD Solvation Model and the M06 Density Functional Family for SAMPL6 Blind Prediction Challenge Molecules. *J. Comput. Aided Mol. Des.* **2020**, *34*, 511−522.
(16) Azarbayjani, A. F.; Aliasgharlou, N.; Khoshbakht, S.; Ghanbarpour, P.; Rahimpour, E.; Barzegar-Jalali, M.; Jouyban, A. Experimental Solubility and Density Functional Theory Studies of Deferasirox in Binary Solvent Mixtures: Performance of Polarizable Continuum Model and Jouyban-Acree Model. *J. Chem. Eng. Data* **2019**, *64*, 2273−2279.
(17) Kolar, M.; Fanfrlik, J.; Lepsik, M.; Forti, F.; Luque, F. J.; Hobza, P. Assessing the Accuracy and Performance of Implicit Solvent Models for Drug Molecules: Conformational Ensemble Approaches. *J. Phys. Chem. B* **2013**, *117*, 5950−5962.
(18) Xu, L. K.; Coote, M. L. Methods To Improve the Calculations of Solvation Model Density Solvation Free Energies and Associated Aqueous pK(a) Values: Comparison between Choosing an Optimal Theoretical Level, Solute Cavity Scaling, and Using Explicit Solvent Molecules. *J. Phys. Chem. A* **2019**, *123*, 7430−7438.
(19) Wu, J. X.; Xu, R. J.; Yuan, X.; Zhao, J.; Wang, J. Equilibrium Solubility of Dinitolmide in Several Neat Solvents and Binary Aqueous Co-solvent Mixtures: Experimental Determination and Thermodynamic Analysis. *J. Chem. Thermodyn.* **2019**, *132*, 373−382.
(20) Eller, J.; Matzerath, T.; van Westen, T.; Gross, J. Predicting solvation free energies in non-polar solvents using classical density functional theory based on the PC-SAFT equation of state. *J. Chem. Phys.* **2021**, *154*, 244106.
(21) Ribeiro, R. F.; Marenich, A. V.; Cramer, C. J.; Truhlar, D. G. Prediction of SAMPL2 Aqueous Solvation Free Energies and Tautomeric Ratios Using the SM8, SM8AD, and SMD Solvation Models. *J. Comput. Aided Mol. Des.* **2010**, *24*, 317−333.
(22) Roese, S. N.; Margulis, G. V.; Schmidt, A. J.; Uzat, C. B.; Heintz, J. D.; Paluch, A. S. A Simple Method to Predict and Interpret the Formation of Azeotropes in Binary Systems Using Conventional Solvation Free Energy Calculations. *Ind. Eng. Chem. Res.* **2019**, *58*, 22626−22632.
(23) Kamlet, M. J.; Abboud, J. L. M.; Abraham, M. H.; Taft, R. W. Linear Solvation Energy Relationships. 23. A Comprehensive Collection of the Solvatochromic Parameters, Pi-Star, Alpha and Beta, and Some Methods for Simplifying the Generalized Solvatochromic Equation. *J. Org. Chem.* **1983**, *48*, 2877−2887.
(24) Cheng, N. L. *Solvent handbook*, 5th ed.; Chemical Industry Press: Beijing, 2014.
(25) Mirzaei, S.; Ivanov, M. V.; Timerghazin, Q. K. Improving Performance of the SMD Solvation Model: Bondi Radii Improve Predicted Aqueous Solvation Free Energies of Ions and pKa Values of Thiols. *J. Phys. Chem. A* **2019**, *123*, 9498−9504.

https://doi.org/10.1021/acsomega.2c02693
ACS Omega 2022, 7, 30920−30929